波 谱 学 杂 志

第 32 卷第 2 期 Vol. 32 No. 2
2015 年 06 月 Chinese Journal of Magnetic Resonance Jun. 2015

Article：1000-4556(2015)02-261-12 doi:10.11938/cjmr20150209

Visualize Diffusion Map of COPD Rat with Hyperpolarized Xenon MRI

RUAN Wei-wei[1,2]，*ZHONG Jian-ping*[1]，*HAN Ye-qing*[1]，*SUN Xian-ping*[1]，
YE Chao-hui[1]，*ZHOU Xin*[1*]

[1. Key Laboratory of Magnetic Resonance in Biological Systems, State Key Laboratory of Magnetic Resonance and Atomic and Molecular Physics, National Center for Magnetic Resonance in Wuhan (Wuhan Institute of Physics and Mathematics, Chinese Academy of Sciences), Wuhan 430071;
2. University of Chinese Academy of Sciences, Beijing 100049]

Abstract：Hyperpolarized ^{3}He or ^{129}Xe diffusion MRI has been demonstrated as a promising technique for the detection of microanatomical changes in chronic obstructive pulmonary disease (COPD). Compared with ^{3}He, ^{129}Xe is more available for the potential clinical applications. However, the measurement of ^{129}Xe apparent diffusion coefficient (ADC) possesses more challenges due to the relevant low gyromagnetic ratio and spin polarization. In this present study, a single *b* value (b = 14 s/cm^2) diffusion-weighted hyperpolarized ^{129}Xe MRI sequence was used to image a balloon phantom, healthy rats, and the COPD rats, respectively. All COPD rats were induced by second-hand smoke and lipopolysaccharide (LPS). The lung ^{129}Xe *ADC* maps were obtained on a 7 T MRI scanner. The mean lung parenchymal ^{129}Xe *ADCs* were 0.044 22±0.002 9 and 0.042 34±0.002 3 cm^2/s (Δ = 0.8/1.2 ms) for the COPD rats, which showed significant increasements in comparison with healthy ones (0.037 7±0.002 3 and 0.036 7±0.001 3 cm^2/s). Furthermore, the corresponding *ADC* histogram of the COPD rats exhibited a broader distribution as compared with the healthy ones. Our experiments demonstrated that the alveolar airspace enlargement in the COPD rats are able to be quantitatively evaluated by hyperpolarized xenon diffusion-weighted MRI.

Key words：hyperpolarized xenon, MRI, lung, ADC, COPD

CLC number：O482.53 **Document code**：A

Received date: 2015-02-11; **Revised date:** 2015-05-10

Foundation item: Gants from the National Natural Science Foundation of China (81227902) and the Chinese Academy of Sciences (KJCX2-EW-N06-04).

Biography: RUAN Wei-wei(1989-), male, born in Hubei, PhD., his research focuses on Hyperpolarized ^{129}Xe MRI of Lungs, Tel.: +86-15927192627, Fax: +86-27-87199291, E-mail: weiweir0812@gmail.com.

*Corresponding author: ZHOU Xin, Tel: +86-27-87198802, E-mail: xinzhou@wipm.ac.cn.

Introduction

Chronic obstructive pulmonary disease (COPD), which is characterized by persistent airflow limitation caused by a mixture of small airways disease (obstructive bronchiolitis) and parenchymal destruction (emphysema), is the fourth-leading cause of death among adults at present[1]. It was predicted to be the fifth burden of disease over the world in 2020[1]. The lung parenchyma contains all levels of bronchia and alveolus, and COPD are progressive destructions of the alveolar walls and subsequent enlargements of alveolar airspaces. The main cause of COPD so far is considered to be smoking, including both heavy smoking and exposure to second-hand smoke[2].

The traditional diagnosis of COPD is based on the pulmonary function testing[3] and clinical symptoms. Conventional pulmonary function tests could reflect the global functional changes, but COPD is a disease that occurs in the changes of pulmonary tissues microstructure. Therefore, pulmonary function tests are insensitive to the initial stages of emphysema[4]. Moreover, high resolution X-ray CT has usually been used to detect abnormal low-attenuating areas of the lung with COPD, but the reduced attenuation may also be caused by other process factors, like smoking-related inflammation or air trapping[5]. Additionally, the potential damage from the high radiation dose of CT scan limits the repeated usage.

Hyperpolarized (HP) ^{3}He and ^{129}Xe gas MRI provide new ways to evaluate both anatomical and functional characteristics of the lungs *in vivo*[5,6]. Hyperpolarized method could enhance ^{3}He or ^{129}Xe magnetic resonance signals by ~10^5 times[7,8], which makes the gases MRI of lungs feasible. In comparison with ^{129}Xe, ^{3}He has a larger gyromagnetic ratio and a higher spin polarization, so it is used in both pre-clinical and clinical researches[10] as a preferred noble gas. However, the limited supply and extremely low natural abundance (~0.013 7%)[10] of ^{3}He prevent it from the extensive applications. Contrarily, ^{129}Xe has a high natural abundance (~26.4%)[10], and it is cheaper because xenon can be acquired by extraction from the air. ^{129}Xe is uniquely suitable for the pulmonary MRI, as it is soluble in the pulmonary tissue and blood, while ^{3}He is not. There are two separate NMR peaks of xenon dissolved in the pulmonary tissue and blood, apart from a peak from the gas phase xenon[10]. Such characters would make ^{129}Xe more popular in future research.

All particles have random translational motion with a velocity called self-diffusion coefficient (D_0). The self-diffusion coefficient of pure ^{129}Xe gases is 0.061 cm^2/s[11]. In the case of unrestricted diffusion in a homogeneous region, the mean particle displacement along a given direction during a duration time (Δ) is given by[11]

$$r = \sqrt{2D_0\Delta} \tag{1}$$

Since the alveolar airspaces have walls or boundaries, the diffusion of gases are restricted. The diffusion coefficients of gases in lungs are different from the self-diffusion coefficients[12], which is called as apparent diffusion coefficient (ADC)**,** and can be measured by diffusion-weighted MRI. The increase of ^{129}Xe ADC values can be observed in emphysematous lungs with respect to that of the healthy ones, due to the enlargements of the

airspaces and destructions of the alveolar walls. Recently, the ADC measurement via hyperpolarized ^{129}Xe MRI has been performed[13,14], which showed an increased ADC of ^{129}Xe in COPD patients as compared with the healthy ones. Because of the non-repeatability and uncontrollability of pathogenesis or severity grades in the COPD patients, it is important to observe and study micro lesions in pulmonary disease model via small animals, like rats or mice. Boudreau and co-workers have used MR spectroscopy to calculate ^{129}Xe ADC of elastase-instilled rats model with emphysema[15]. However, to our best knowledge, there is no report about ^{129}Xe ADC distribution map in the lung of COPD rat model induced by both lipopolysaccharide and smoking.

The purpose of this study was to determine whether hyperpolarized ^{129}Xe diffusion-weighted MRI with a single *b* value could detect the microstructural changes in the lungs of COPD rats compared with the healthy ones. The self-diffusion coefficient of hyperpolarized ^{129}Xe has been measured in a balloon phantom to confirm the accuracy of the pulse sequences. The ^{129}Xe ADC distribution maps of COPD rat lungs and the corresponding histograms have been obtained, and the mean lung parenchymal ^{129}Xe ADC was calculated. In this present study, the comparison between COPD rats and the healthy ones has also been discussed.

1 Materials and methods

1.1 ^{129}Xe polarization and delivery

Natural abudance Xe (26.4% ^{129}Xe) was polarized ~20% by a homebulit xenon polarizer with the technique of spin-exchange optical pumping (SEOP). The gas mixture consisted of 2% Xe, 10% N_2, and balanced ^{4}He. Nitrogen could quench the fluorescence of Rb atoms, and helium could pressure-broaden the Rb D_1 profile to absorb most of the laser power[16].

Firstly, Rb electron spin polarization was induced via a standard optical pumping process, i.e., a 794.7 nm laser from a 75 W diode laser array resonates with Rb D1 transition line. Then, hyperpolarized ^{129}Xe gas was produced by spin-exchange collision with the optically pumped Rb atoms. We developed a device for accumulating the hyperpolarized Xe, which is called hyperpolarized xenon colllecting system. It consists of a cold trap immersed in a liquid nitrogen Dewar, which is surrounded by a permanet magnet of 0.22 T. Hyperpolarized Xe was frozen over the walls of the cold trap, while the residual gases (nitrogen and helium) flew away due to the lower freezing points. With such procedure, 180 mL HP Xe gas could be obtained in 30 min. After collection, the cold trap was placed in a bath with boiling water, thawing HP Xe ice into gas rapidly. Finally, a Tedlar bag containing hyperpolarized ^{129}Xe was connected to a homebuilt ventilator.

1.2 Animal preparation

Eight female Sprague Dawley (SD) rats (Animal Laboratory of Wuhan University, China) were used. The experimental group (five rats, each 300±60 g) received 0.2 mL of lipopolysaccharide (LPS, Company, Sigma, America, 1 mg/mL) by the endotracheal

instillation every two weeks (Day 1 and Day 14)[17], and the rats were exposed to cigarettes smoke for 1 h/day from Day 2 to Day 28 (6 times per day except Day 14). The control group (three rats, each 300±100 g) received neither LPS nor smoke.

Each rat was initially anaesthetized with 5.0% of isoflurane (Keyuan Pharmaceutical, Shandong, China), and then intubated with an 1.628 mm endotracheal tube, which is tied to the trachea. After the intubation, the rat was ventilated by the homebuilt ventilator, which is computer-controlled using a self-desinged software based on the LabVIEW. Fig. 1 shows the schematic diagram-of the timing sequence for ventilation and MRI acqusitions. The rats were alternatively ventilated with oxygen and hyperpoarized xenon. For the ventilation of O_2, the breath rate was set to 50 breaths per minute with an inspiratory time of 400 ms and an expiratory time of 800 ms. The peak inspiratory pressure was 12 cm H_2O, with an inspiratory capacity of about 2.5 mL per breath. After 5 min, the concentration of isoflurane was turned down to 2% for maintenance. For the ventilation of hyperpolarized ^{129}Xe, the breath rate was set to 17 breaths per minute, with an inspiratory time 500 ms, a breath-hold time of 2 000 ms and an expiratory time of 1 000 ms. The peak inspiratory pressure was 15 cm H_2O, with an inspiratory capacity about 3.0 mL per breath.

The MRI acquisitions were triggered synchronously at the beginning of the breath-hold (arrow in Fig. 1). Immediately before an MRI acquisition, flushing three times with hyperpolarized ^{129}Xe gas was used to take away the oxygen in tubes as much as possible. After MRI acquisitions, rats were ventilated to regularly breathe O_2 again.

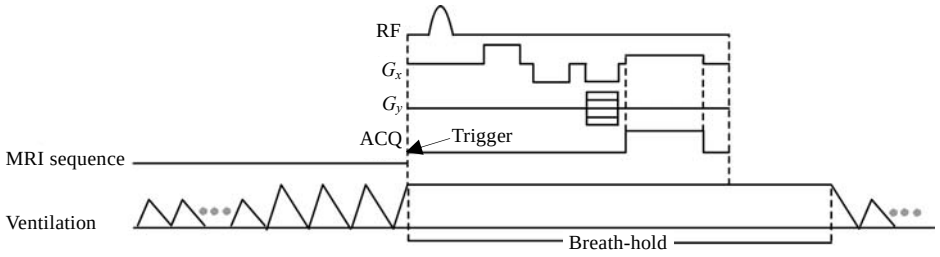

Fig. 1 The schematic diagram of timing sequence for ventilation and MRI acquisitions

1.3 MRI and data Analysis

The protocol for measuring ADC was a gradient-echo based pulse sequence, including a bipolar gradient waveform in one of the three directions for diffusion sensitization, as shown in Fig. 2. The *b*-values were given by[18]

$$b = \gamma^2 G^2 [\delta^2 (\Delta - \frac{\delta}{3}) + \tau(\delta^2 - 2\Delta\delta + \Delta\tau - \frac{7}{6}\delta\tau + \frac{8}{15}\tau^2) \quad (2)$$

where γ is the gyromagnetic ratio of ^{129}Xe; G is the maximum gradient amplitude; τ is the ramp time of gradient, which was 0.123 ms in our experiments; δ is the gradient pulse width; and Δ is the diffusion time, which is a crucial parameter. It was selected according to the characteristic diffusion length (r) in Eq. (1). The r should be larger than the average alveolar

radius, so the diffusion of ^{129}Xe atoms will be restricted due to the alveolar walls or boundaries. We set δ = 0.65 ms, Δ = 0.8 ms and 1.2 ms, so the characteristic diffusion length were 97.98 μm and 120 μm, respectively, which are larger than the average alveolar length, 70 μm, of the healthy rats[15]. The *b*-value was 0 s/cm^2 and 14 s/cm^2. The calculation of ADC is given by[5,11]

$$S_{14} = S_0 \cdot \exp(-b \cdot ADC) \tag{3}$$

where S_0 and S_{14} are the signal amplitudes of each pixels of MR images, with b = 0 s/cm^2 and b = 14 s/cm^2, respectively. The S_0 map and S_{14} map were acquired in the separate breath-holds in order to enhance the SNR. To avoid the effect of T_1 relaxation of hyperpolarized ^{129}Xe during the interval time of acquiring $S_0$1 map and S_{14} map, another $S_0$2 map was acquired after the S_{14} map. The interval time from acquiring $S_0$1 map to $S_0$2 map was pretty short in comparison to the T_1 of ^{129}Xe in the Tedlar bag, so that S_0 could be given by

$$S_0 = (S_0 1 + S_0 2)/2 \tag{4}$$

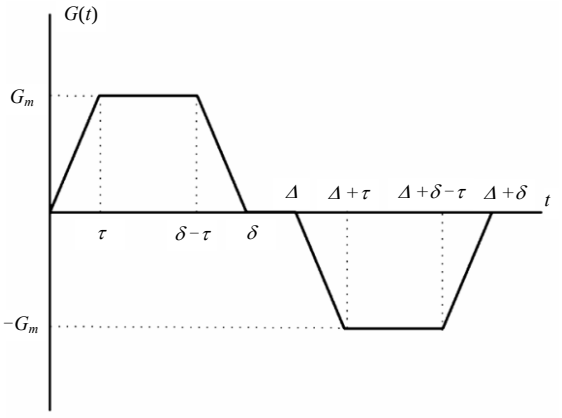

Fig. 2 The bipolar gradient waveform used to sensitize the diffusion of ^{129}Xe gas

All MR studies were performed on a 7 T animal MRI scanner (Bruker BioSpec 70/20 USR) with maximal gradients of 444.75 mT/m. Two homebuilt birdcage radio frequency coils with diameters of 5.5 and 7.5 cm, both tuned to ^{129}Xe (83.07 MHz) frequency, were used for rats with different weights. The parameters of rat diffusion weighted MRI were: a matrix size of 48×48, a field of view of 6×6 cm^2, a flip angle of 13°, a BW of 50 kHz, and a slice thickness of 100 mm; for Δ = 0.8 ms, *TE*/*TR* = 3.3/13.0 ms; and for Δ = 1.2 ms, *TE*/*TR* = 3.7/13.0 ms; the whole acquisition time for one image is 624 ms.

The diffusion of gases in a balloon is almost unrestricted, so the ADC measured in a balloon phantom should approximate the self-diffusion coefficient (D_0). We set the MRI parameters in phantom experiments identical to that of *in vivo* experiments.

All MR data were analyzed using Matlab. All images were generated from MRI *K*-spaces by two-dimensional discrete Fourier transform (DFT), and then the outlines of

lungs were profiled by the threshold segmentation. The ADC maps were calculated by the Eq. (3) and (4). The major airways were removed by setting an appropriate ADC threshold**.** During the calculation of mean values of ADC in the lungs, only the ADC values between 0 cm^2/s and 0.14 cm^2/s were retained[7]. In addition, the representative ADC maps shown in Fig. 3 and Fig. 4 were zero-filled to 96×96 in *K*-spaces.

1.4 Morphology observation

After MRI experiments, rats were sacrificed. Then, the lungs were extracted to be made into H&E-stained histological sections. Each H&E-stained histological section was 10 micrometer and observed through the microscope (Nikon Eclipse Ts 100). The pulmonary mean linear intercept (*Lm*) was calculated based on the H&E-stained histological sections and a paired student *t*-test was performed for statistical comparison between COPD rats and the healthy ones for Lm by Excel (Office 2013).

2 Results

2.1 Phantom experiments

Fig. 3 shows the measured self-diffusion coefficient map of hyperpolarized ^{129}Xe in a balloon phantom and the corresponding histogram. The measured value of the self-diffusion coefficient was 0.062 4 ± 0.022 5 cm^2/s, which is consistent with values obtained previously[5,15,19,20]. It confirmed that this approach is robust to measure the *ADC* of ^{129}Xe. A slight increase of *ADC* in the phantom is probably owing to the existing of other gases (like O_2 or N_2) in the balloon.

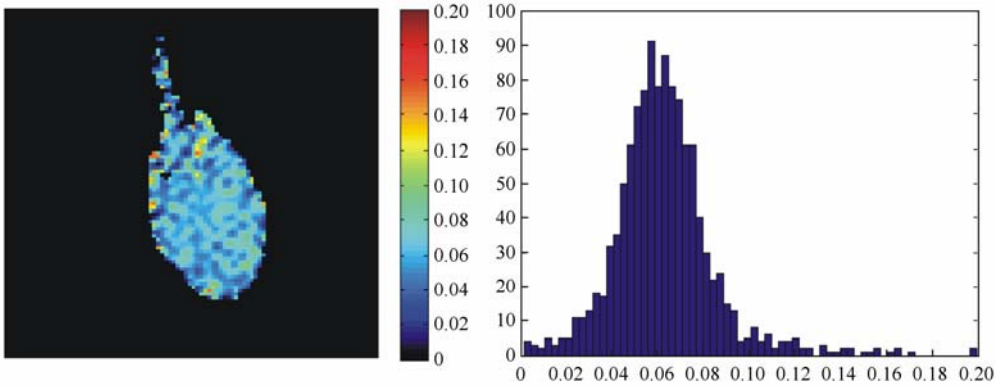

Fig. 3 The measured self-diffusion coefficient map of hyperpolarized ^{129}Xe in a balloon phantom (left) and the corresponding histogram (right). The measured value of the self-diffusion coefficient in the balloon phantom is 0.062 4±0.022 5 cm^2/s (b = 14 s/cm^2, Δ = 0.8 ms). The histogram of the *ADC* presents a Gaussian distribution

2.2 *In vivo* experiments

Table 1 lists the mean values of the lung parenchymal *ADC* and the standard deviations at two different diffusion times (0.8 ms and 1.2 ms) for all rats used in the study, including

three healthy rats and five COPD rats. Results indicate that the mean *ADC* values of lung parenchymal in healthy rats were significantly lower than the values of COPD rats except the COPD rat 5, whose value was almost the same as that of healthy rat 3. Meanwhile, a slight decrease of the mean *ADC* could be found when increasing the diffusion time from 0.8 ms to 1.2 ms among all rats.

Table 1 The *ADC* values of three healthy rats and five COPD rats. Each row lists the mean *ADC* values of lung parenchyma at two diffusion times (0.8 ms and 1.2 ms)

Animal	*ADC*/(cm^2/s)	
	Δ = 0.8/ms	Δ = 1.2/ms
healthy rat 1	0.0353±0.0019	0.0349±0.0015
healthy rat 2	0.0378±0.0019	0.0357±0.0015
healthy rat 3	0.0399±0.0019	0.0375±0.0008
COPD rat 1	0.0458±0.0032	0.0428±0.0042
COPD rat 2	0.0464±0.0022	0.0454±0.0004
COPD rat 3	0.0428±0.0019	0.0408±0.0022
COPD rat 4	0.0463±0.0012	0.0433±0.0023
COPD rat 5	0.0398±0.0007	0.0394±0.0006

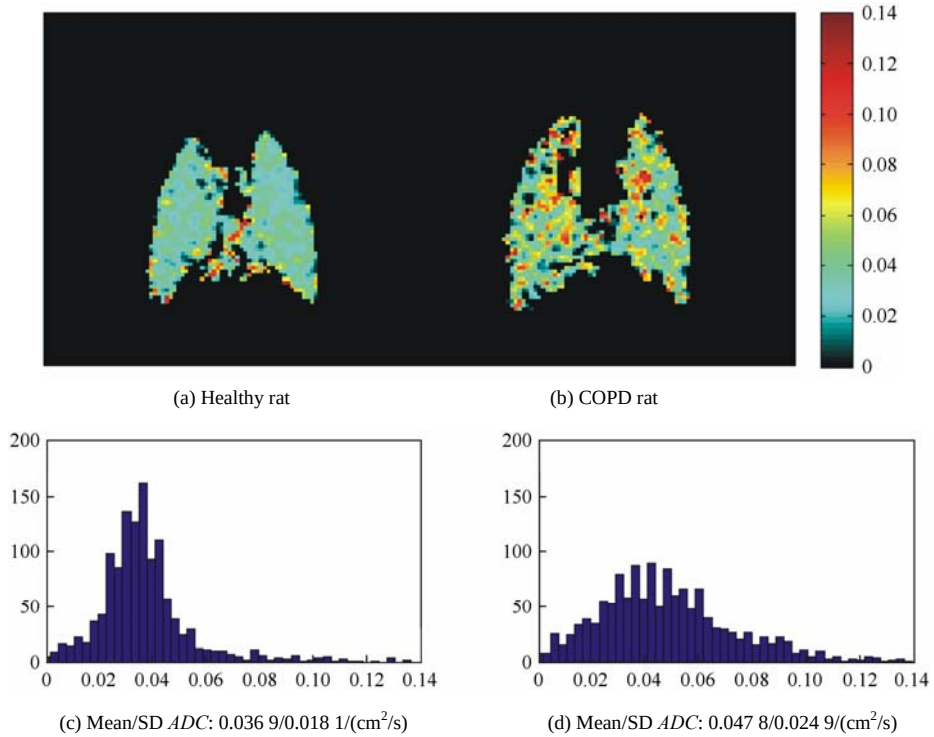

(a) Healthy rat (b) COPD rat

(c) Mean/SD *ADC*: 0.036 9/0.018 1/(cm^2/s) (d) Mean/SD *ADC*: 0.047 8/0.024 9/(cm^2/s)

Fig. 4 The representative ^{129}Xe *ADC* maps of the lung parenchymal *ADC* maps and corresponding *ADC* histograms in a single measurement: (a) A representative healthy rat with low mean lung parenchymal *ADC* of 0.036 9±0.018 1 cm^2/s (Δ = 0.8 ms) , indicating a normal alveolar microstructure. (b) A representative COPD rat with a high mean lung parenchymal *ADC* of 0.047 8±0.024 9 cm^2/s (Δ = 0.8 ms), indicating an enlarged alveolar microstructure. (c) The *ADC* histogram of a healthy rat exhibits an almost homogeneous distribution. (d) The *ADC* histogram of a representative COPD rat exhibits a moderately broader distribution

Fig. 4 shows the difference of ^{129}Xe lung parenchymal *ADC* maps and the corresponding *ADC* histograms in a single measurement between a representative healthy rat and a representative COPD rat (Δ = 0.8 ms). The mean lung parenchymal *ADC* of the representative COPD rat is 0.047 8±0.024 9 cm^2/s, which is significantly higher than that of the healthy one (0.036 9±0.018 1 cm^2/s). Furthermore, the corresponding *ADC* histogram of the representative COPD rat exhibits a broader distribution, while that of the healthy rat exhibits an almost homogeneous distribution.

2.3 Morphology

Table 2 lists the mean linear intercept (*Lm*) for the COPD rats and healthy rats and the corresponding *p* value. The mean linear intercept of 80.24±8.09 μm for COPD rats was significantly larger than that of 62.07±4.02 μm for health rats ($p < 0.05$). The increased Lm represented the destructive and enlarged alveoli for COPD rats. Fig. 5 shows the corresponding H&E-stained histological sections of the lungs for the healthy rat (left) and the COPD rat (right) used in Fig. 4. Enlarged alveolar airspaces are clearly visible in the COPD rat compared with the healthy one.

Table 2 The mean linear intercept (*Lm*) for the COPD rats and healthy rats

	COPD rats	Healthy rats	
Lm/μm	80.24±8.09	62.07±4.02	p = 0.0054

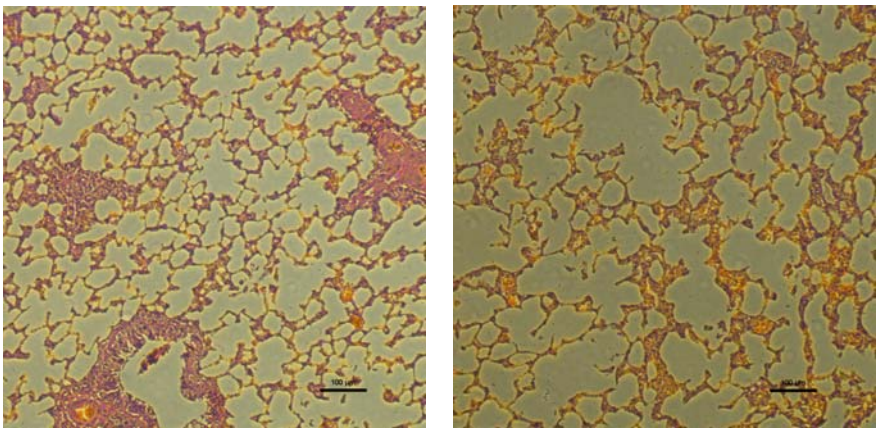

Fig. 5 The corresponding H&E-stained histological sections of the lungs for the healthy rat (left) and the COPD rat (right) used in Fig. 4. The magnification was 100. The enlarged airspaces in the COPD rat lung can be easily identified

3 Discussion

MRI measurements of hyperpolarized ^{3}He or ^{129}Xe gas diffusion in the lung airspaces have been demonstrated to be a useful way to provide unique information about the lung microstructure at the alveolar level[15,21–25]. In comparison with ^{3}He, hyperpolarized ^{129}Xe gas

diffusion-weighted MRI poses several challenges. The lower diffusivity of ^{129}Xe requires a larger *b*-value to achieve a sufficient weighting, which means that a stronger gradient or a longer diffusion time are needed[21,26]. However, the stronger gradient or the longer diffusion time will accelerate the singal decay of hyperpolarized ^{129}Xe signal. Moreover, the a nearly 3-fold lower gyromagnetic ratio of ^{129}Xe and the lower spin polarization in comparison with ^{3}He would result in a lower image SNR[27]. In comparison with the study of humans, the volume of hyperpolarized ^{129}Xe used in rat lung studies is almost 300 times smaller because of the much smaller volume of animal lungs[15,21,28,29]. These factors create a significant challenge for hyperpolarized ^{129}Xe gas diffusion-weighted MRI of the rat lungs.

In comparison with the multiple *b*-values to fit the ADC of hyperpolarized ^{129}Xe in the rat lungs, the experiment with a single *b*-value has less requirements about the polarization of hyperpolarized ^{129}Xe[21]. The mean lung parenchymal ^{129}Xe *ADC* of 0.044 22±0.002 9 cm^2/s (Δ = 0.8 ms) and 0.042 34±0.002 3 cm^2/s (Δ = 1.2 ms) in five COPD rats showed a significant increase relative to three healthy ones, i.e., 0.037 7±0.002 3 cm^2/s (Δ = 0.8 ms) and 0.036 7±0.001 3 cm^2/s (Δ = 1.2 ms). The increased ^{129}Xe ADC values reflected the erosion of alveolar walls in COPD rats[21,30], which was consistent with the results from H&E-stained histological sections. The destruction can also be reflected by the inhomogeneous distribution of ADC map and the corresponding histogram, as shown in Fig. 4. If a high enough polarization of hyperpolarized ^{129}Xe is obtained, the *ADC* map with high resolution may directly reflect the erosive destruction location of alveolus.

In the present study, the mean ^{129}Xe *ADC* values of the lung parenchyma have a slight decrease with increasing the diffusion time from 0.8 ms to 1.2 ms. As the mean ADCs can reflect relative airspace sizes, the slight decrease can be attributed to the increase in the number of ^{129}Xe atom collisions with airspace walls, reducing the mean displacement of the atoms during the diffusion time[31]. This phenomenon is consistent with the previous ^{3}He study[31], and the optimal diffusion time should be explored further. In addition, there is no distinct difference of the mean ^{129}Xe *ADCs* between the COPD rat 5 and the healthy rat 3. A possible reason is the self-recovery of the damaged lung in COPD rat 5. To attain sufficient image SNR, the lung image with (S_{14}) and without ($S_0$1 and $S_0$2) gradient were acquired using separate breath-holds. Any difference of lung position, gas volume or gas composition among the three breath-holds could change the signal intensity of each image, and it would influence the mean ADC values, accordingly[15]. In the future study, the lung images may be acquired in a single breath-hold through either the use of enriched ^{129}Xe or the achievement of a higher spin polarization.

4 Conclusion

The experiments demonstrated that despite the lower gyromagnetic ratio and lower polarization of ^{129}Xe relative to ^{3}He, hyperpolarized ^{129}Xe diffusion weighted MRI with a

single *b* value is able to detect the changes in the lungs of COPD rats compared with the healthy ones. The alveolar airspace enlargement in the COPD rats could be reflected by the increase of mean ^{129}Xe *ADC* of the lung parenchyma and the broader distribution of the corresponding histogram. In short, hyperpolarized ^{129}Xe MRI shows a great potential for the detection and characterization of early emphysematous changes in the lungs of COPD.

Acknowledgement: This work was supported by the Natural Science Foundation of China (81227902) and the Chinese Academy of Sciences (KJCX2-EW-N06-04).

Reference:

[1] Rabe K F, Hurd S, Anzueto A, *et al*. Global strategy for the diagnosis, management, and prevention of chronic obstructive pulmonary disease - GOLD executive summary[J]. Am J Resp Crit Care Med, 2007, 176(6): 532－555.

[2] Wang C B, Mugler J P, de Lange E E, *et al*. Lung injury induced by secondhand smoke exposure detected with hyperpolarized helium-3 diffusion MR[J]. J Magn Reson Imaging, 2014, 39(1): 77－84.

[3] Plotkowiak M, Burrowes K, Wolber J, *et al*. Relationship between structural changes and hyperpolarized gas magnetic resonance imaging in chronic obstructive pulmonary disease using computational simulations with realistic alveolar geometry[J]. Philos T Roy Soc A, 2009, 367(1 896): 2 347－2 369.

[4] Thurlbeck W M. Overview of the pathology of pulmonary-emphysema in the human[J]. Clin Lab Med, 1984, 4(3): 539－559.

[5] Yablonskiy D A, Sukstanskii A L, Quirk J D, *et al*. Probing lung microstructure with hyperpolarized noble gas diffusion MRI: theoretical models and experimental results[J]. Magn Reson Med, 2014, 71(2): 486－505.

[6] Driehuys B, Cofer G P, Pollaro J, *et al.* Imaging alveolar-capillary gas transfer using hyperpolarized ^{129}Xe MRI[J]. Proc Natl Acad Sci USA, 2006, 103(48): 18 278－18 283.

[7] Albert M S, Cates G D, Driehuys B, *et al.* Biological magnetic-resonance-imaging using laser polarized ^{129}Xe[J]. Nature, 1994, 370(6 486): 199－201.

[8] Li H D, Zhang Z Y, Han Y Q, *et al.* Lung MRI using hyperpolarized gases[J]. Chinese J Magn Reson, 2014, 31(3): 307－320.

[9] Mata J, Altes T, Truwit J, *et al.* Characterization and detection of physiologic lung changes before and after placement of bronchial valves using hyperpolarized ^{3}He MR imaging: preliminary study[J]. Acad Radiol, 2011, 18(9): 1 195－ 1 199.

[10] Moller H E, Chen X J, Saam B, *et al.* MRI of the lungs using hyperpolarized noble gases[J]. Magn Reson Med, 2002, 47(6): 1 029－1 051.

[11] Yablonskiy D A, Sukstanskii A L, Leawoods J C, *et al.* Quantitative *in vivo* assessment of lung microstructure at the alveolar level with hyperpolarized ^{3}He diffusion MRI[J]. Proc Natl Acad Sci USA, 2002, 99(5): 3 111－3 116.

[12] Habib D, Grebenkov D, and Guillot G, *et al.* Gas diffusion in a pulmonary acinus model: experiments with hyperpolarized helium-3[J]. Magn Reson Imaging, 2008, 26(8): 1 101－1 113.

[13] Kaushik S S, Cleveland Z I, Cofer G P, *et al.* Diffusion-weighted hyperpolarized ^{129}Xe MRI in healthy volunteers and subjects with chronic obstructive pulmonary disease[J]. Magn Reson Med, 2011, 65(4): 1 155－1 165.

[14] Kirby M, Svenningsen S, Kanhere N, *et al.* Pulmonary ventilation visualized using hyperpolarized ^{3}He and ^{129}Xe magnetic resonance imaging: differences in COPD and relationship to emphysema[J]. J Appl Phys, 2013, 114(6): 707－715.

[15] Boudreau M, Xu X, Santyr G E, *et al.* Measurement of ^{129}Xe gas apparent diffusion coefficient anisotropy in an elastase-instilled rat model of emphysema[J]. Magn Reson Med, 2013, 69(1): 211－220.

[16] Zhou X, Mazzanti M L, Chen J J, *et al.* Reinvestigating hyperpolarized relaxation time in the rat brain ^{129}Xe longitudinal with noise considerations[J]. NMR Biomed, 2008, 21(3): 217－225.

[17] Li S W, Zhang L, Li C L, *et al.* Fumigation and intratracheal instillation of lipopolysaccharide or they combining ozone exposure for establishing COPD models in rats[J]. J Beijing Univ Tradit Chin Med, 2014, 37(5): 321－324.

[18] Mattiello J, Basser P J, Lebihan D, *et al.* Analytical expressions for the *b*-matrix in NMR diffusion imaging and spectroscopy[J]. J Magn Reson Ser A, 1994, 111(2): 232－232.

[19] Blackberg L, Metsanurk E, Tamm A, *et al*. Molecular dynamics study of xenon on an amorphous Al_2O_3 surface[J]. Nuclear Instrum Methods Phys Res Sect A, 2014, 759: 10－15.

[20] Chen X J, Moller H E, Chawla M S, *et al*. Spatially resolved measurements of hyperpolarized gas properties in the lung *in vivo*. Part I: Diffusion coefficient[J]. Magn Reson Med, 1999, 42(4): 721－728.

[21] Ouriadov A, Farag A, Kirby M, *et al.* Lung morphometry using hyperpolarized ^{129}Xe apparent diffusion coefficient anisotropy in chronic obstructive pulmonary disease[J]. Magn Reson Med, 2013, 70(6): 1 699－1 706.

[22] Carrero-Gonzalez L, Kaulisch T, Ruiz-Cabello J, *et al.* Apparent diffusion coefficient of hyperpolarized ^{3}He with minimal influence of the residual gas in small animals[J]. NMR Biomed, 2012, 25(9): 1 026－1 032.

[23] Halaweish A F, Hoffman E A, Thedens D R, *et al.* Effect of lung inflation level on hyperpolarized He apparent Diffusion coefficient Measurements in never-smokers[J]. Radialogy, 2012, 268(2): 572－580.

[24] Diaz S, Casselbrant I, Piitulainen E, *et al.* Validity of apparent diffusion coefficient hyperpolarized ^{3}He MRI using MSCT and pulmonary function tests as references[J]. Eur J Radiol, 2009, 71(2): 257－263.

[25] Patz S, Muradyan I, Hrovat M I, *et al.* Diffusion of hyperpolarized ^{129}Xe in the lung: a simplified model of ^{129}Xe septal uptake and experimental results[J]. New J Phys, 2011, 13(1): 015009.

[26] Sukstanskii A L, Yablonskiy D A. Lung morphometry with hyperpolarized ^{129}Xe: theoretical background[J]. Magn Reson Med, 2012, 67(3): 856－866.

[27] Kirby M, Svenningsen S, Owrangi A, *et al.* Hyperpolarized ^{3}He and ^{129}Xe MR imaging in healthy volunteers and patients with chronic obstructive pulmonary disease[J]. Radiology, 2012, 265(2): 600－610.

[28] Nouls J, Fanarjian M, Hedlund L, *et al.* A constant-volume ventilator and gas recapture system for hyperpolarized gas MRI of mouse and rat lungs[J]. Concepts Magn Reson Part B Magn Reson Eng, 2011, 39B(2): 78－88.

[29] Shukla Y, Wheatley A, Kirby M, *et al.* Hyperpolarized ^{129}Xe magnetic resonance imaging: tolerability in healthy volunteers and subjects with pulmonary disease[J]. Acad Radiol, 2012, 19(8): 941－951.

[30] Fricker M, Deane A, Hansbro P M, *et al.* Animal models of chronic obstructive pulmonary disease[J]. Expert Opin Drug Dis, 2014, 9(6): 629－645.

[31] Gierada D S, Woods J C, Bierhals A J, *et al.* Effects of diffusion time on short-range hyperpolarized ^{3}He diffusivity measurements in emphysema[J]. J Magn Reson Imaging, 2009, 30(4): 801－808.

超极化 Xenon 对慢阻肺的可视化加权成像

阮伟伟[1,2]，钟俭平[1]，韩叶清[1]，孙献平[1]，叶朝辉[1]，周 欣[1*]

[1. 武汉磁共振中心，波谱与原子分子物理国家重点实验室，中国科学院生物磁共振分析重点实验室（中国科学院 武汉物理与数学研究所），武汉 430071；
2. 中国科学院大学，北京 100049]

摘 要：超极化气体 ^{3}He 或者 ^{129}Xe 扩散加权成像已经被证明了能够有效检测慢性阻塞性肺部疾病(COPD)中肺部微结构的改变．相比于 ^{3}He，^{129}Xe 更便宜而且更容易获得，但是 ^{129}Xe 成像中较低的信噪比致使 ^{129}Xe 的肺部表面扩散系数(ADC)的测量面临着许多困难．在该研究中，为了得到更高的图像信噪比，作者对气球模型，健康大鼠和 COPD 大鼠进行了单个 *b* 值(14 cm^2/s)的扩散加权超极化 ^{129}Xe 磁共振成像(MRI)．所有的 COPD 模型大鼠是通过烟熏和注射内毒素(LPS)进行诱导得到的．在 7 T 磁共振成像仪上面获得了大鼠肺实质的超极化 ^{129}Xe *ADC* 值分布图．COPD 大鼠肺实质的 ^{129}Xe *ADC* 值是 0.044 22±0.002 9 和 0.042 34±0.002 3 cm^2/s (Δ = 0.8/1.2 ms)，远大于健康大鼠肺实质的 ^{129}Xe *ADC* 值 0.037 7±0.002 3 和 0.036 7±0.001 3 cm^2/s．而且 COPD 大鼠肺实质相关的 ^{129}Xe *ADC* 直方图也表现出了一定的展宽．这些结果说明了 COPD 大鼠肺泡空腔的增大能够通过 ^{129}Xe 在肺里面的 *ADC* 增长和相关直方图的拓宽反应出来，从而证明了单个 *b* 值的扩散加权 MRI 方法可以有效地对 COPD 大鼠进行检测．

关键词：超极化氙气；磁共振成像；肺；表面扩张系数；慢阻肺

*通讯联系人：周欣，电话：+86-27-87198802，E-mail: xinzhou@wipm.ac.cn.